Fundamental Understanding of Dynamic Interfacial Phenomena in Solid State Batteries

Xingcheng Xiao (PI), Qinglin Zhang

General Motors Global R&D Center

Brian Sheldon, Yue Qi

Brown University

Yang-Tse Cheng, Ambrose Seo

University of Kentucky

June 24, 2021

This presentation does not contain any proprietary, confidential, or otherwise restricted information

Project ID # BAT 488

gm RESEARCH & DEVELOPMENT

DESIGN BUILD SELL

THE WORLD'S BEST VEHICLES

Overview

Timeline

- Project start date: 10/1/2019
- Project end date: 12/31/2022
- Percent completed: 45%

Barriers addressed

- High interfacial impedance caused by side reaction, mechanical incompatibility, and stress.

Budget

- Total project funding: $ 1,333,325
  - DOE share: $ 1,000,000
  - Contractor share: $ 333,325
- Funding received in FY2017: $188,560
- Funding for FY2020: $552,119

Partners

Interactions/ collaborations

- Brown University
- University of Kentucky

Project lead: General Motors

Relevance

- Most failures in solid state battery is associated with interfaces between electrodes and solid electrolyte, due to the coupled mechanical and chemical degradation.
- The dynamic evolution of the mechanical/transport property and structure/composition of the interfaces has not been fully understood, due to the challenges on the characterization of interfacial mechanical properties, such as elastic modulus, interfacial strength, and fracture toughness.
- A well-controlled platform combining with in situ characterization is needed to conduct fundamental investigations of the coupled dynamic mechanical/chemical properties.

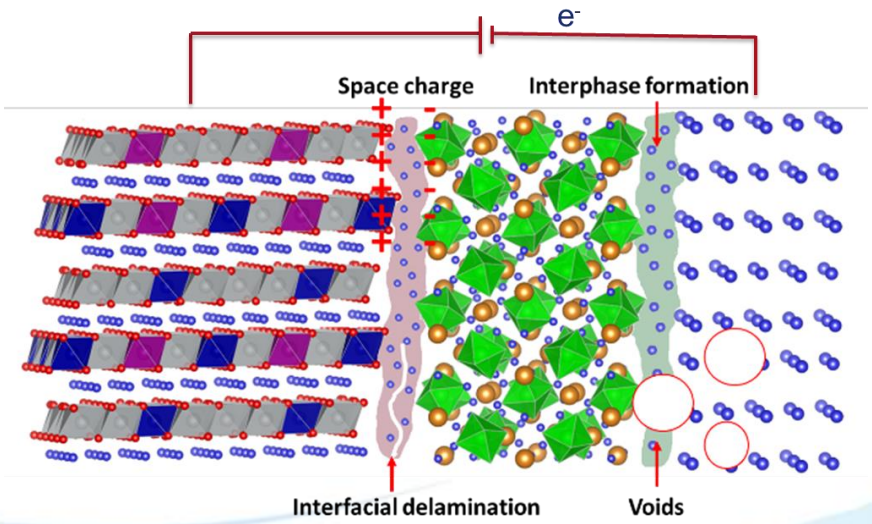

Project Milestones

Month/ Year	Milestone of Go/No-Go Decision	Status
March. 2020	The film electrode system can reliably adapt to different in situ electrochemical tests and long-term cycle performance tests.	**completed**
June 2020	The thin film electrodes, including LLZO and LiPON, with the comparable ionic conductivity to the reported values.	**completed**
Sept. 2020	in situ electrochemical-mechanical tools which enable the characterization of critical mechanical properties associated with interfaces. A rank of the interfacial adhesion between Li and different SEs.	**Completed**
Dec. 2020	Make Go/No-Go decision based on whether in situ and ex situ experiments and simulation data to be complimentary and coherent.	**Completed**

Approach/Strategy

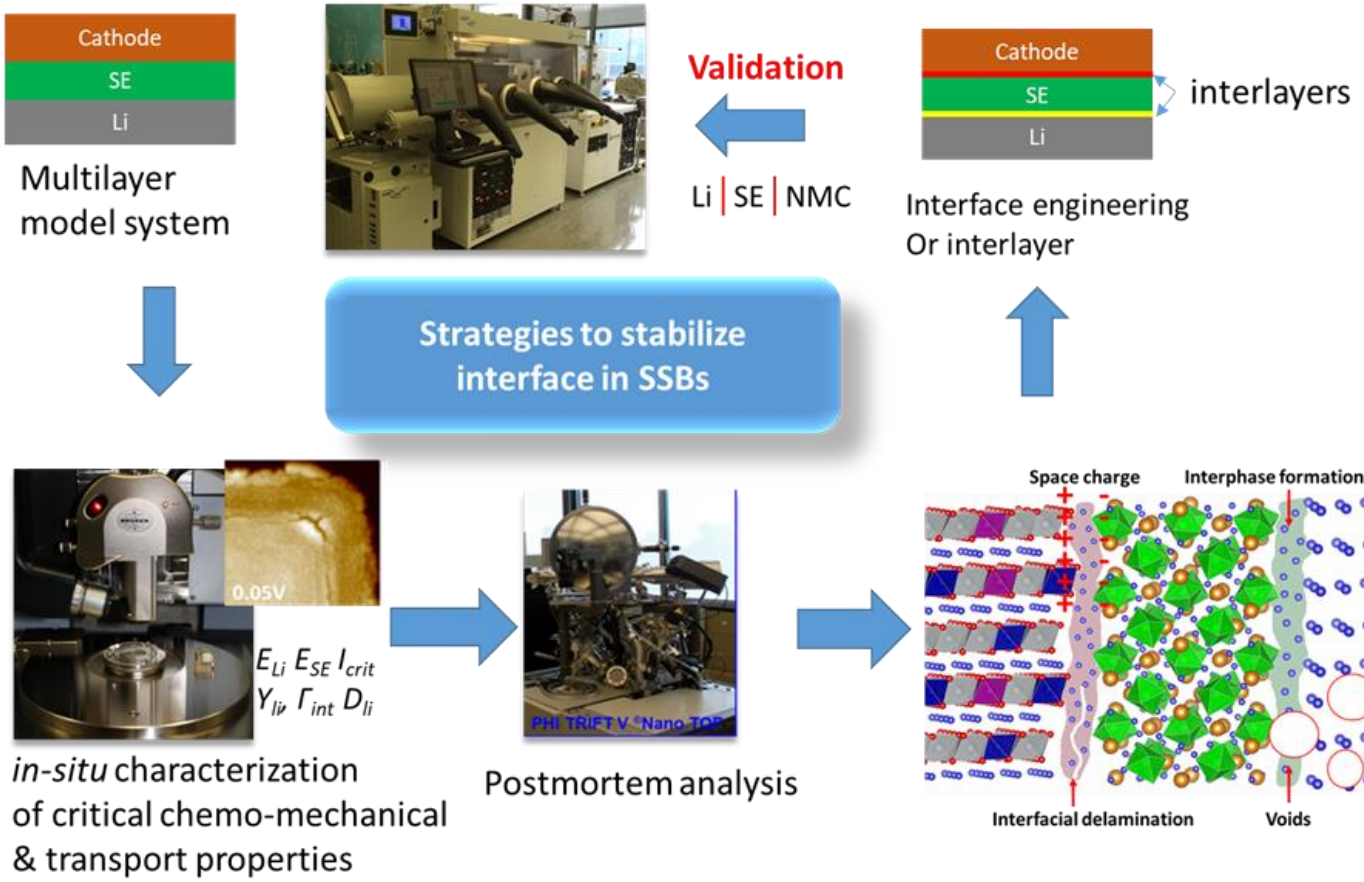

- Develop a model system to identify critical mechanical/chemical/transport properties related with interfaces.
- Establish a multi-dimensional property map to correlate mechanical failure mechanisms, morphology, and cycle efficiency, and provide a design guidance for developing the desirable artificial interlayers.

Accomplishment 1: developed reliable model systems and In-situ techniques to investigate interface dynamic phenomena

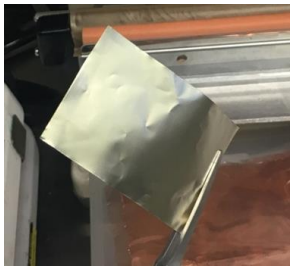

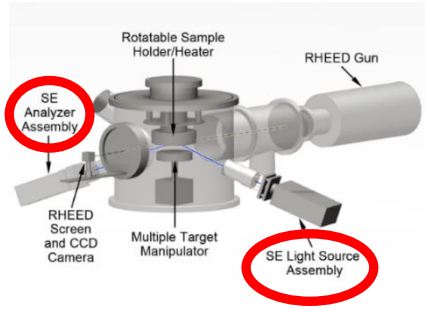

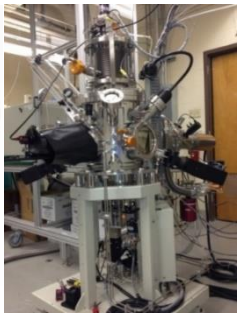

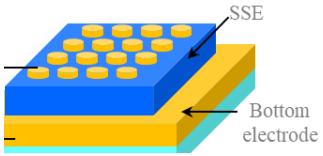

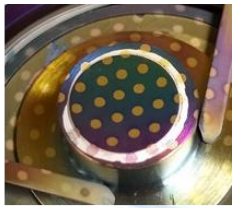

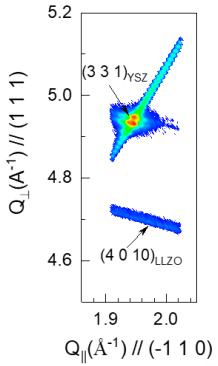

Thin film deposition system for SSB model system

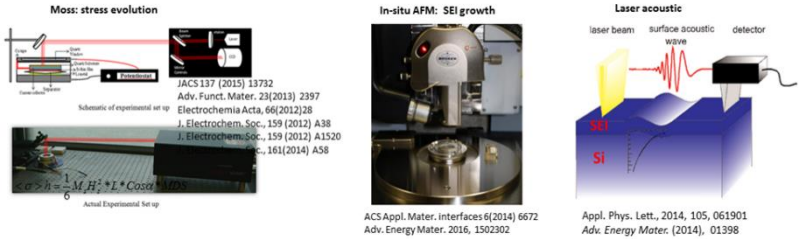

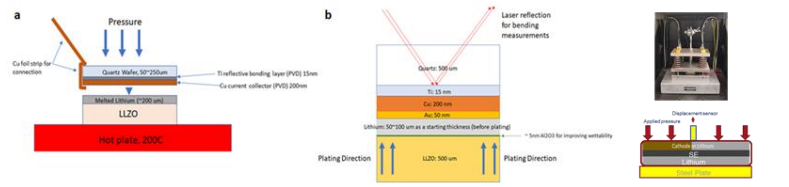

In-situ techniques to investigate the mechanical behavior of SSB system

Accomplishment 2: developed a model system to investigate the stress evolution in solid electrolyte at initial stage

BROWN
School of Engineering

Sheldon's group

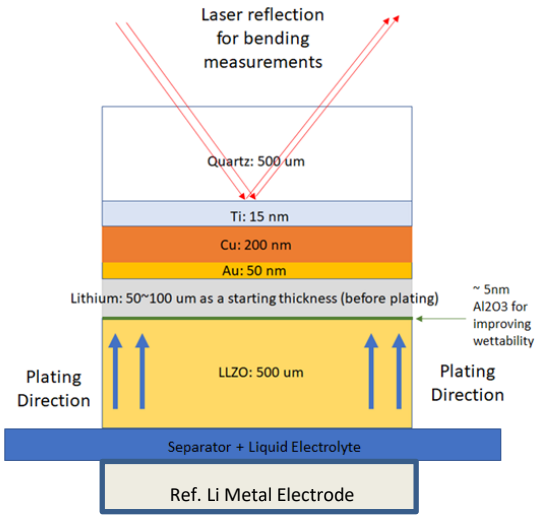

Objective: To Investigate dynamic stress evolution in LLZO during plating using in-situ curvature measurements

Stresses that can be generated during Li plating/ stripping:

1. **Stress at the Li/LLZO interface**
2. **Stress from local defects within LLZO (including Li dendrites)**
3. **Growth stress in Li metal (small based on previous work)**

Stress from 1 and 2 will produce measurable bending.

Are these stresses related to dendrite formation ?

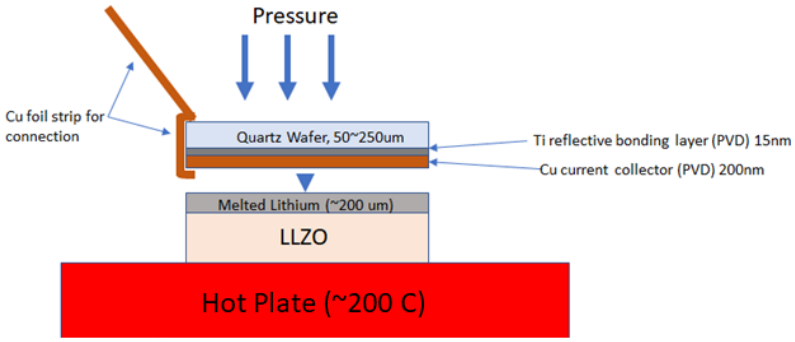

Information to probe:

1. Tensile or compressive stress ?
2. Stress magnitude
3. Correlation with electrochemical measurements

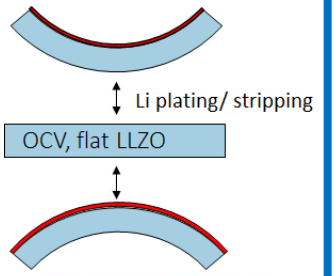

LLZO prepared by Dr. Kunjoong Kim (Jennifer Rupp's group, MIT)

Accomplishment 2.1: investigated the stress evolution in solid electrolyte during initial plating process

BROWN
School of Engineering

Sheldon's group

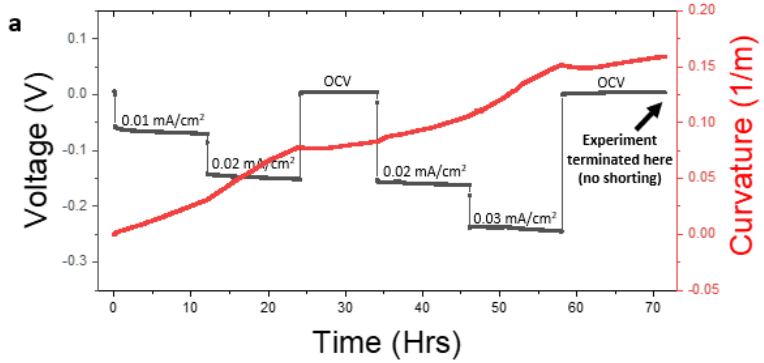

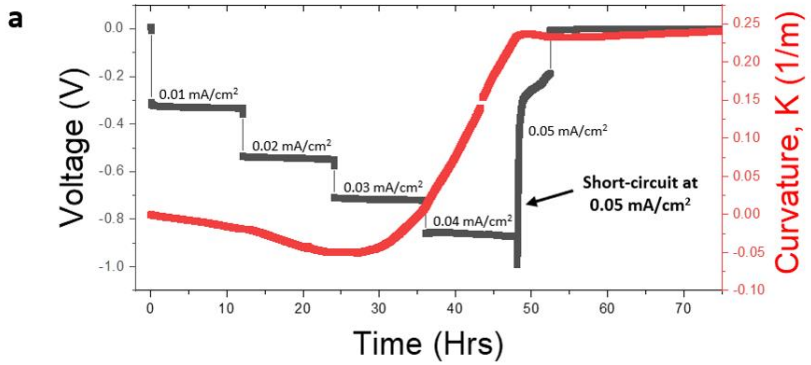

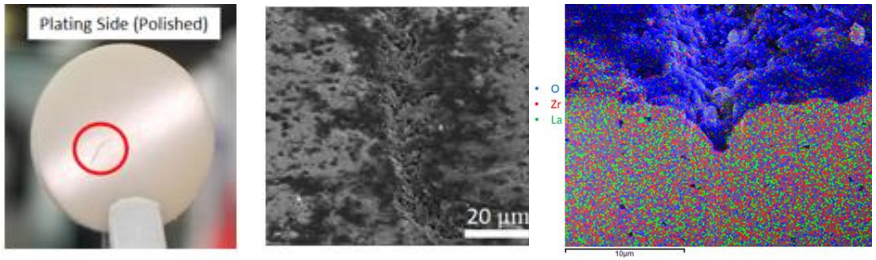

no shorting

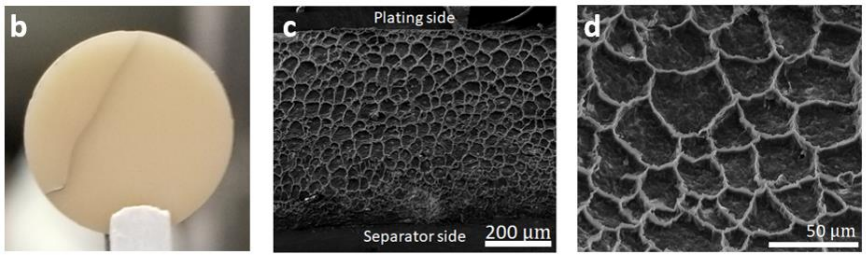

with shorting

- As the amount of plated lithium and current density increases - significant increase in curvature
- Partial lithium penetration on the plating side of the LLZO pellet occurs before short circuit
- Post-mortem analysis shows that short occurs via lithium metal penetration along the grain boundaries

Accomplishment 2.2: Interpretation of the stress evolution in LLZO

BROWN
School of Engineering

Sheldon's group

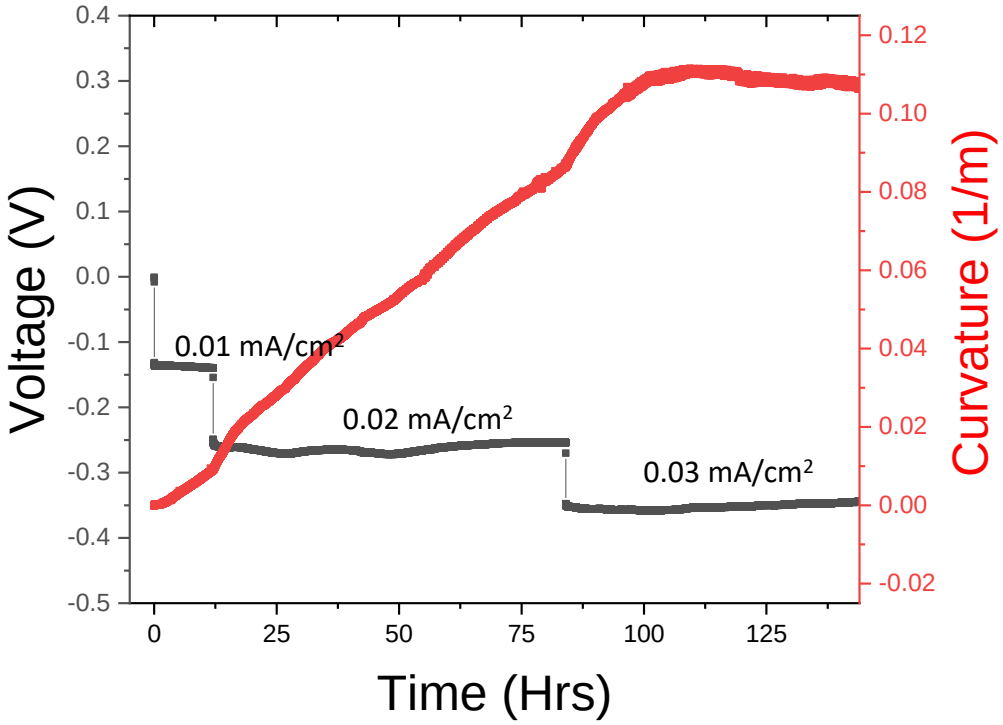

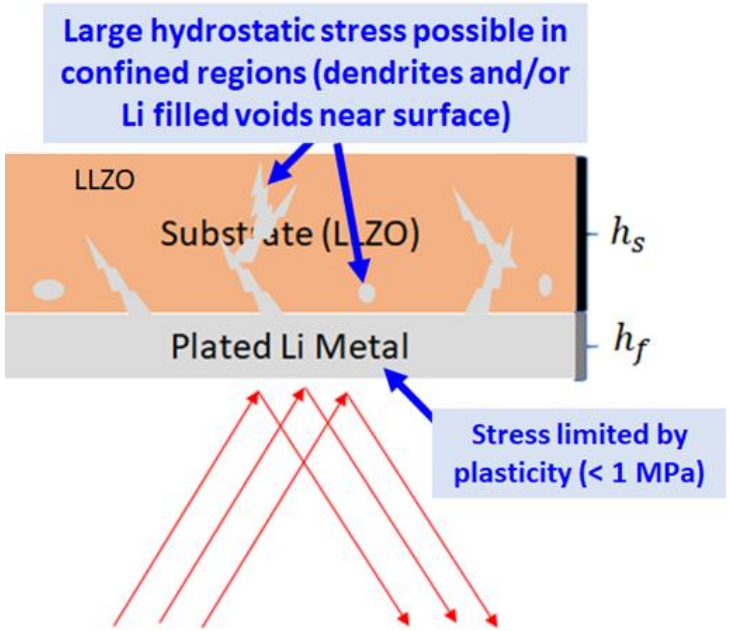

- Steady-state curvature (i.e., stress state) is reached at longer times
- Proposed explanation: steady-state condition is associated with steady-state stresses and stabilization of Li metal / LLZO interface during initial plating
- This stabilization contributes to the Increasing curvatures during shorter experiments (i.e., during galvanostatic and OCV holds)

Accomplishment 3.1: Developed and integrated in situ nanoindentor to investigate mechanical behaviors of LLZO

Cheng's group

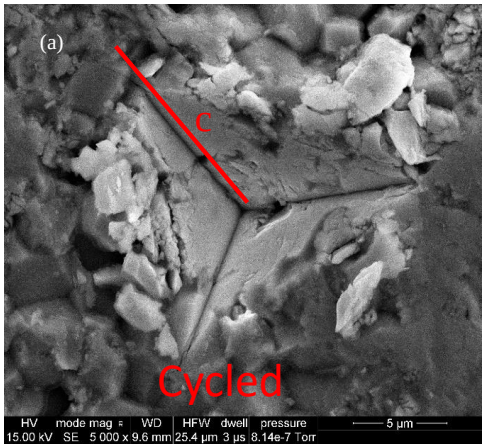

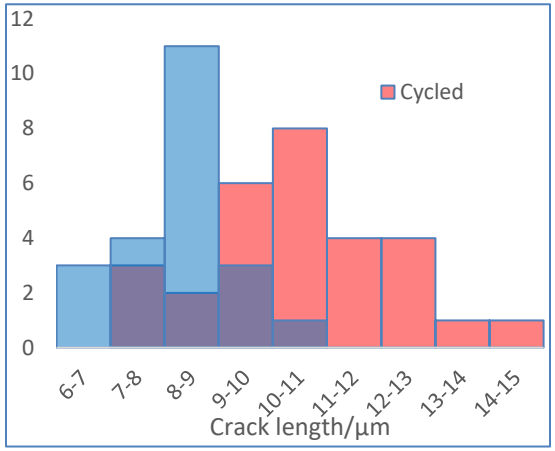

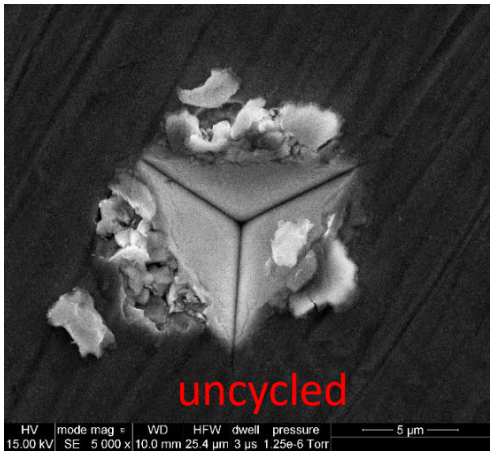

Specimens	Fracture Toughness/MPa√m	Crack Length/μm	Modulus/GPa	Hardness/GPa	H/E
Uncycled	2.25 ± 0.41	8.26 ± 0.96	84.3 ± 4.4	7.1 ± 0.7	0.084 ± 0.005
Cycled	1.80 ± 0.54	10.49 ± 1.67	87.1 ± 13.1	5.6 ± 1.8	0.062 ± 0.012

$$K_c = \alpha \left(\frac{E}{H}\right)^{1/2} \left(\frac{P}{c^{3/2}}\right)$$

K_c = Fracture toughness
E = Elastic modulus
H = Hardness
c = Crack length
P = Max load
α = Indenter tip constant (0.032)

- Nanoindentation inside an argon-filled glovebox.
- SEM imagining to measure crack length and mode of fracture.
- Electrochemical cycling degrades the mechanical properties of LLZO, due to the Li plating along the grain boundaries.

Accomplishment 3.2: developed in situ pressure cell to investigate the impact of stack pressure

Cheng's group

- Made a Li|LLZTO|Li pouch cell and applied a 1.81 MPa (262.5 psi) pressure for < 1 min.
- Tested electrochemical impedance spectroscopy (EIS) under several conditions
  - Medium Pressure is about 0.66 MPa (95.72 psi)
  - Large Pressure is about 1.44 MPa (208.85 psi)

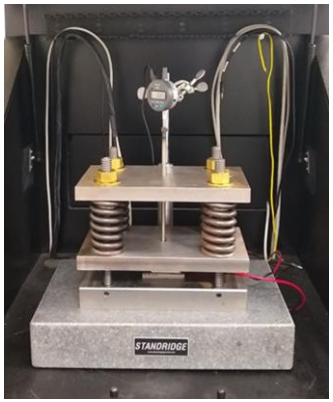

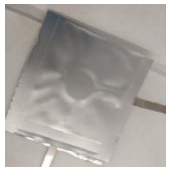

Condition	Estimated Contact Resistance/Ohm
No pressure	*NA*
0.66 MPa	90,000
1.44 MPa	6,400
Pressure Removed	800

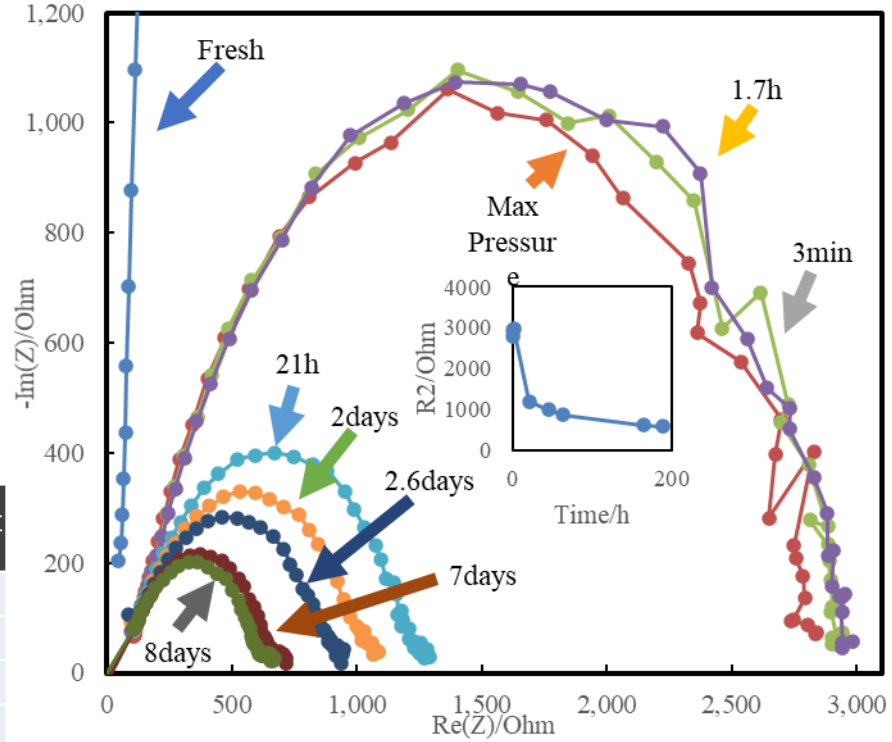

- Pressure affects the initial contact resistance
- The contact resistance improves even after pressure was removed and improves without needing to go to high loads (>10MPa)
- Creep behavior of Li metal leading to plastic flow, maximizing the contact area.

Accomplishment 4.1: investigated vacancy formation along the interfaces between Li and different compounds

BROWN
School of Engineering
Qi's group

	Li(001)/Li_2O(110)	Li(001)/Li_2PO_2N(010)	Li(111)/Li_3N(001)	Li(001)/LLZO(001)	Li(001)/Li_2CO_3(001)	Li(001)/LiF(001)
charge transfer	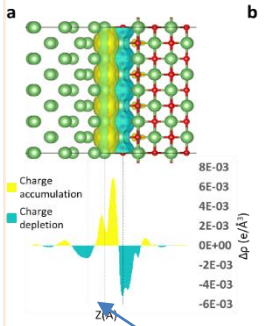	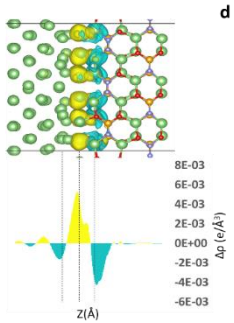	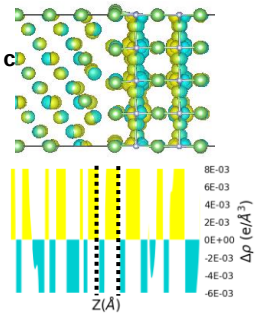	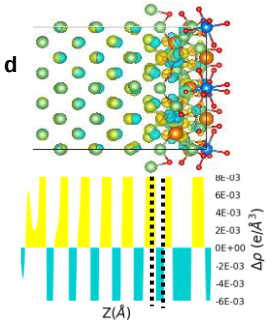	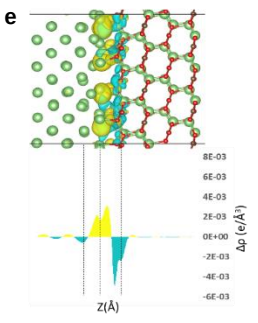	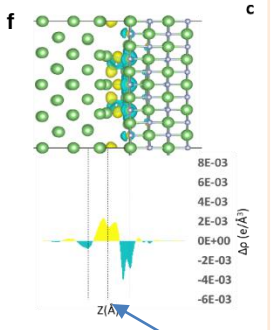
V_{Li}	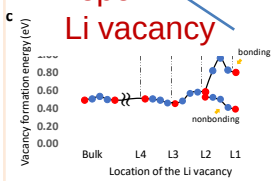 Repel Li vacancy	The Li/Li_2O and Li/LiF impact the vacancy formation energy in the first 2 layers of the Li slab.				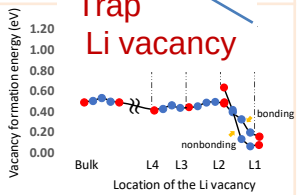 Trap Li vacancy
W_{ad}	1.11 J/m²	0.64 J/m²	0.78 J/m²	0.76 J/m²	0.30 J/m²	0.28 J/m²
θ:	0°	55.9°	56.9	60.2°	105.7°	108.7°
	Wetting				Non-wetting	

Li_3N: the main decomposed products in the Li/Li_2PO_2N interface
LLZO: intensively studied solid electrolyte in experiments

Accomplishment 4.2: identified the impact of surface charges of SE on Li vacancy formation energy.

BROWN School of Engineering
Qi's group

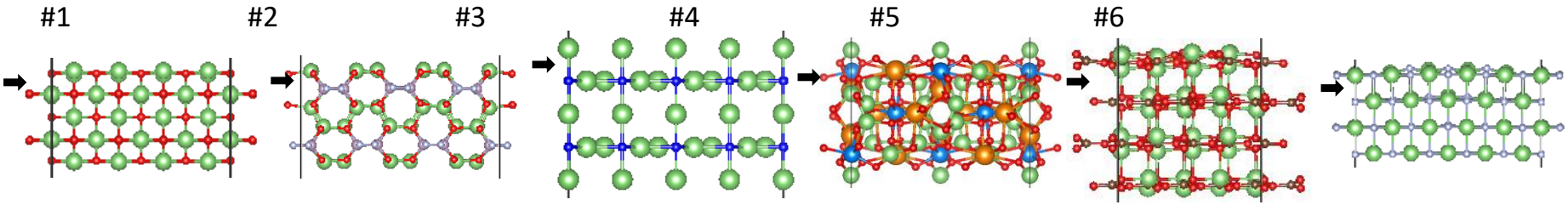

#	Surface	Slab formula	Termination (C_{sur})	Net charge	Surface charge (top 3Å)	Wetting	V_{Li}^0 trapping
1	Li_2O(110)	$Li_{120}O_{60}$	Stoichiometric	0	0	Y (0°)	Repel
2	Li_2PO_2N(010)	$Li_{72}P_{36}O_{72}N_{36}$	Stoichiometric	0	-2	Y (55.9°)	?
3	Li_3N 001	$Li_{112}N_{32}$	Li_8	+8	+16	Y (56.9°)	Trap
4	LLZO Zr r 001	$Li_{32}La_{16}Zr_{12}O_{64}$	$Li_2La_2Zr_2O_8$	0	+2	Y (60.2°)	Trap
5	Li_2CO_3(001)	$Li_{64}C_{32}O_{96}$	Stoichiometric	0	0	N (105.7°)	?
6	LiF(001)	$Li_{100}F_{100}$	Stoichiometric	0	0	N (108.7°)	Trap

Ionic formal charge
Li: +1, O: -2, F: -1, P: +5, N: -3, C:+4, La: +3, Zr: +4.
The black arrow indicates the top 3Å-region on the surface.

- The low Li vacancy formation energy may be due to the positive charges on Li_3N (001, Li) and the LLZO (001, Zr-rich) surfaces
- Will investigate the Li vacancy generation at Li/SE interfaces with negative surface charges (i.e. other Li_2PO_2N surfaces, Li, N terminated Li_3N surfaces).

stable LLZO surfaces and its interface with Li

BROWN
School of Engineering
Qi's group

#1 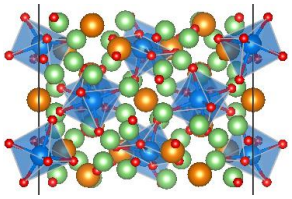

Zr poor (001) O

#2 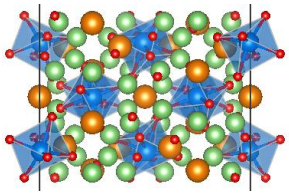

Zr poor (001)

#3 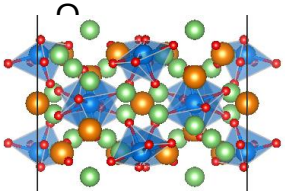

Zr rich (001) O

#4 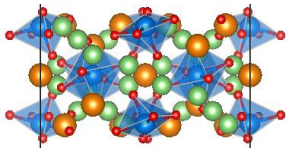

Zr rich (001)

#5 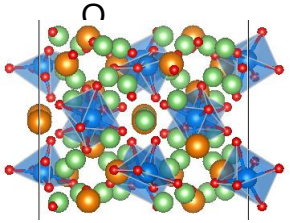

Zr poor (100)

#6 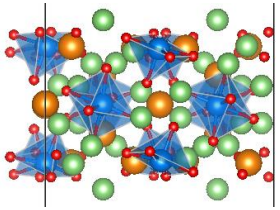

Zr rich (100)

Li: light green, La: brown, Zr: light blue, O: red.

#	Surface	Formula	Termination (C_{sur})	Υ (J/m²)	Ref[1] (J/m²)
1	Zr p 001	$Li_{48}La_{20}Zr_{12}O_{78}$	Li_3LaO_3	0.83	0.82
2	Zr p 001 O	$Li_{48}La_{20}Zr_{12}O_{80}$	Li_3LaO_4	1.35	
3	Zr r 001	$Li_{32}La_{16}Zr_{12}O_{64}$	$Li_2La_2Zr_2O_8$	0.93	0.92
4	Zr r 001 O	$Li_{28}La_{16}Zr_{12}O_{64}$	$La_2Zr_2O_8$	1.58	
5	Zr p 100	$Li_{44}La_{20}Zr_{12}O_{76}$	$LiLaO_2$	0.83	0.74
6	Zr r 100	$Li_{32}La_{16}Zr_{12}O_{64}$	$Li_2La_2Zr_2O_8$	0.88	0.83

[1] *ACS Appl. Mater. Interfaces*. **2020**,*12*,16350−16358.

Slab	X-axis	Y-axis
Li (001)	13.744	13.744
LLZO (001)	13.134	13.134
Strain	-4.64 %	-4.64 %

The Zr rich (001) (#3) slab was used to build the interface due to **more under-coordinated O on the surface** and small lattice mismatch with the 4x4 Li (001) slab.

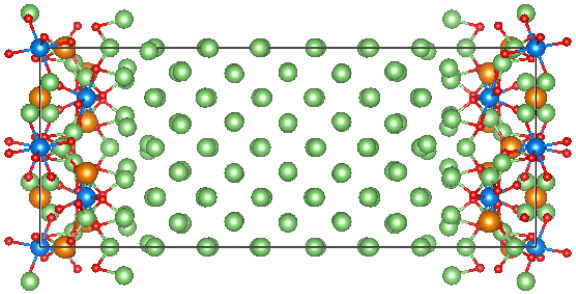

Li(001)/LLZO Zr rich (001) interface

Li/LLZO	Υ_{form} (J/m²)	W_{adh} (J/m²)	$\Upsilon_{Li(001)}$ (J/m²)	cos(θ)	Θ (°)
Li(001)/LLZO Zr rich (001)	0.76	0.63	0.42	0.496	60.2

Accomplishment 5.1. developed a nanocomposite interlayer for Li/SE

Our approach: A solution-based approach to form a compliant artificial SEI layer which consists of Li_3PO_4 and $LiNO_3$ on lithium metal. (Patent application filed)

Li foil

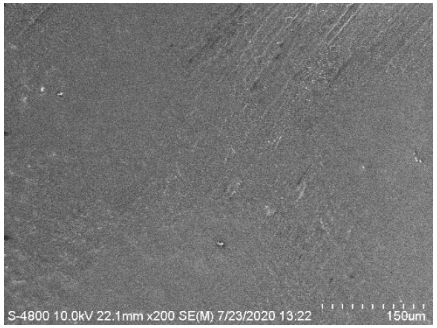

With composite polymer coating

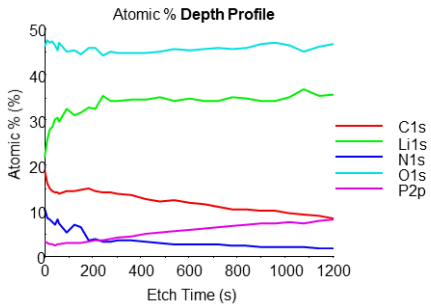

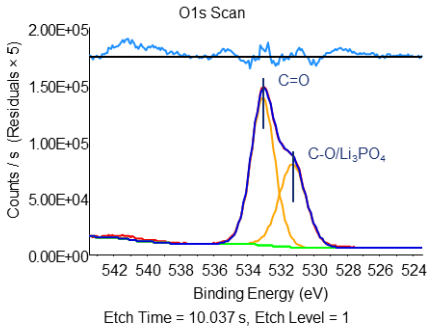

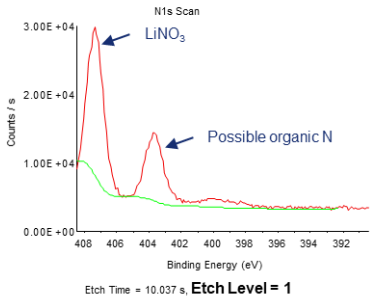

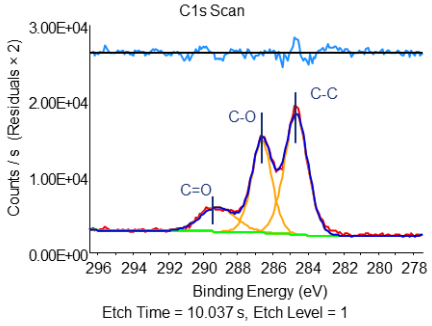

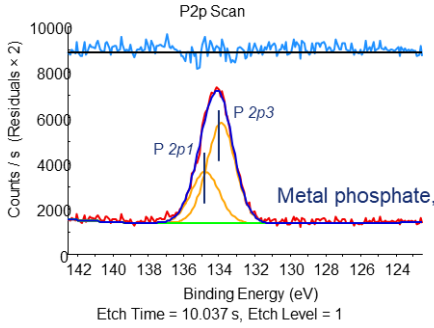

Li_3PO_4 and $LiNO_3$ are embedded in the organic matrix to protect Li metal

Accomplishment 5.2. investigated the impact of the interlayer on mechanical stability of interface between LAGP and Li (Micro-CT)

Micro-CT

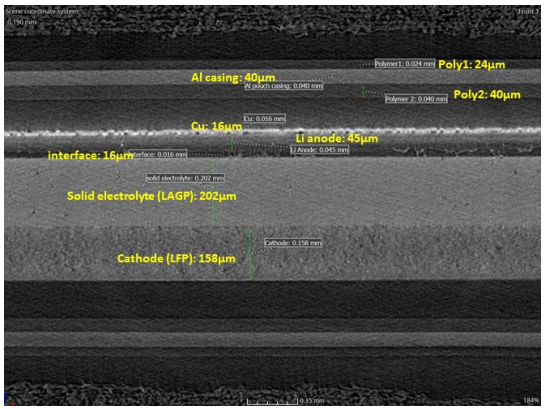

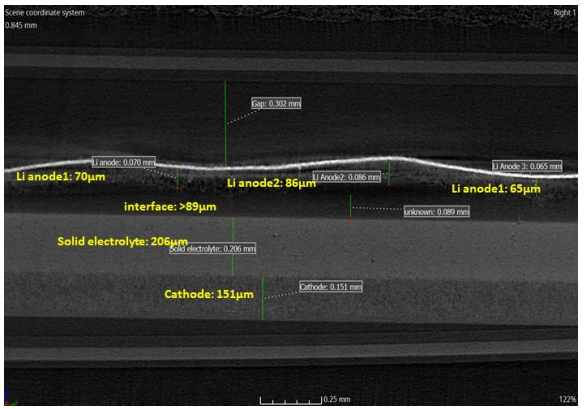

XPS analysis on SE after cycling

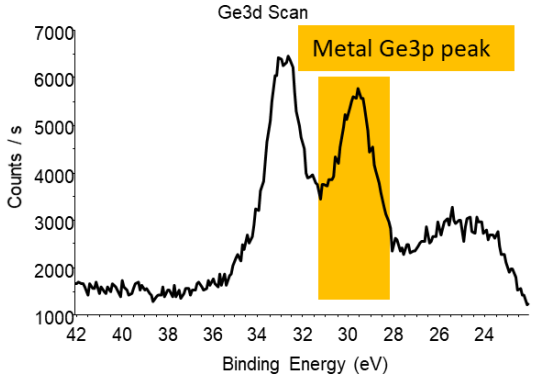

LAGP surface cycled with control lithium

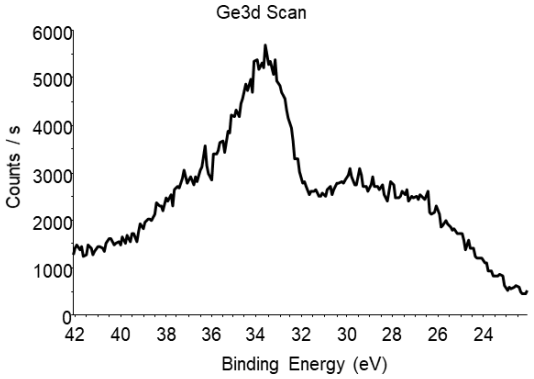

LAGP surface cycled with coated lithium

- The composite interlayer prevents the reaction between Li and LAGP, retains good contact, and avoids the interfacial resistance increase.
- For controlled sample, the reduced product, metallic Ge can be detected on the surface of LAGP SE facing Li metal anode. No metallic Ge was detected on the LAGP surface facing coated metal Li anode.

Accomplishment 5.2. developed a nanocomposite interlayer to enhance the long-term cycle stability of LLZO based SSBs.

❑ **50um Li electrode; LLZTO solid electrolyte (700 um)**

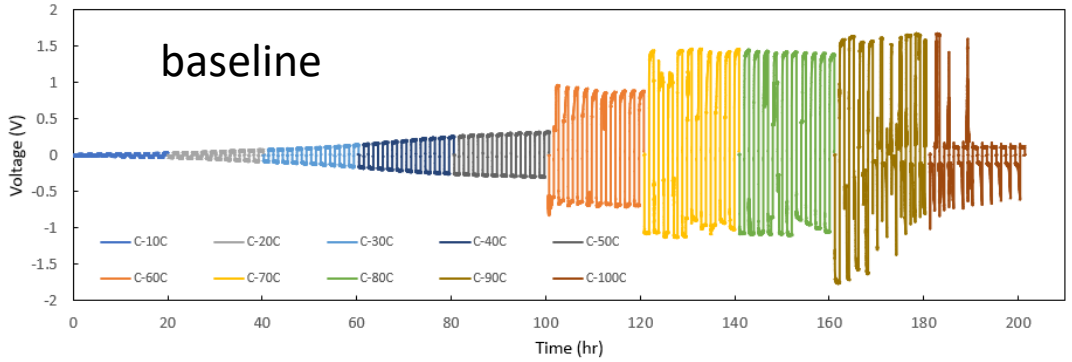

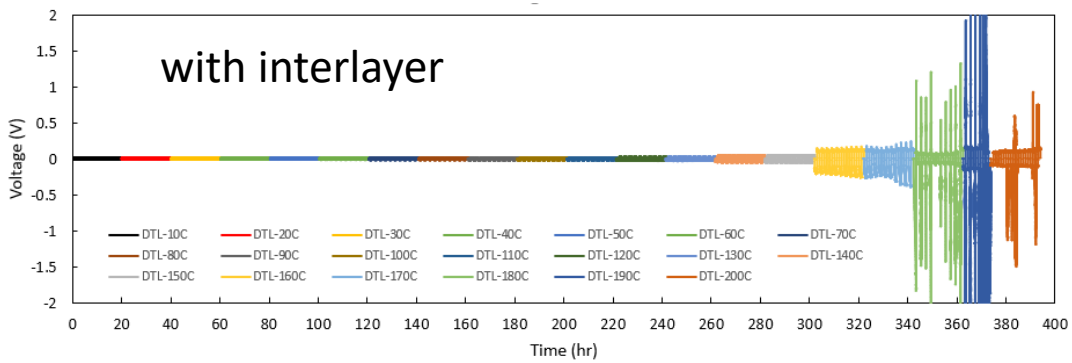

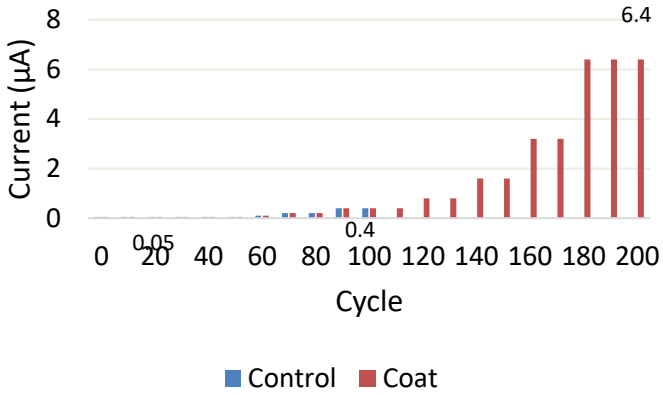

- Control and Coated sample were under same cycle condition in Swagelok cell in the initial 100 cycles
- Coated sample survived another 100 cycles with a high current of 6.4μA
- Control sample is shorted at a current of 0.4μA.
- Coated sample is shorted at a current of 6.4μA.

- The composite interlayer maintains good contact between Li and LLZO and avoids the interfacial resistance increase.

Conclusions

- Various coating deposition techniques, in situ techniques, and postmortem analysis capabilities have been developed to understand the interfacial dynamic phenomena in solid state batteries. LLZO thin films have been successfully deposited on various substrates. Different configurations of electrode/SSE/electrode structures have been proposed to measure properties such as ionic conductivities.
- Curvature change during plating reveals that the bending which occurs is too large to be caused by only the plated lithium, and significant stress occurs in the solid electrolyte. The Li plating along the grain boundaries and onset of Li penetration induces significant compressive stress in the LLZO, leading to the mechanical degradation of LLZO. The latter is consistent with in-situ nanoindentation results.
- Mechanical properties of solid electrolyte may degrade upon electrochemical cycling. Real-time monitoring of the mechanical properties of solid electrolyte may provide early warning signs before lithium dendrites short circuiting. External pressure intermittently applied may heal contacts between lithium metal and solid electrolyte to achieve low interface impedance.
- Further developed DFT-KMC model to investigate the interfacial strength and vacancy evolution between Li and different SE. Demonstrated the role of coating interface on controlling Li morphology evolution during delithiation. The Li/LLZO interface is wetting with a reasonable high Work of adhesion, however, it still traps Li vacancies which may be related to the surface termination of LLZO interfaces with higher cation concentrations and thus positive charge.
- A more mechanically flexible and ion conductive composite interlayer has been developed which can significantly reduces the interfacial impedance and extend cycle life.

Responses to Previous Year Reviewers' Comments

- New project started on 1/1/2020.
- Not reviewed last year.

Collaborations and Coordination with Other Institutions

Dr. Wu Xu Dr. Chongmin Wang, (PNNL)	Investigate the stability of artificial SEI on Li using *in-situ* TEM; Advanced electrolyte additives;
Prof. Jennifer L. M. Rupp Dr. Kunjoong Kim(MIT)	Synthesis and characterization of LLZO electrolyte

Remaining challenges and barriers

- Lack of reliable approach to characterize the interfacial fracture strength between Li metal and solid electrolyte.
- How to calculate the stress based on curvature measurement? Need finite element analysis.
- How to incorporate stack pressure effect, while the length-and-time scale for Li creep is beyond typical atomistic modeling (KMC and MD) time scale.
- Understanding the mechanisms responsible for the observed changes in mechanical properties of solid electrolyte and developing effective mitigation strategies to maintain mechanical integrity.

Publications and presentations

Publications

1. Y. Wang, D. Dang, X. Xiao, Y.-T. Cheng, Structure and mechanical properties of electroplated mossy lithium: Effects of current density and electrolyte, Energy Storage Materials, Vol. 26, 2020, Pages 276-282.
2. C. Yang, Y. Lin; B. Li, X. Xiao, Y. Qi, The Bonding Nature and Adhesion of Polyacrylic Acid (PAA) Coating on Li-metal for Li Dendrite Prevention, ACS Appl. Mater. Interfaces 2020, 12, 45, 51007–51015
3. Cho, J. H.; Xiao, X.; Guo, K.; Liu, Y.; Gao, H.; Sheldon, B. W., Stress evolution in lithium metal electrodes. Energy Storage Materials 2020, 24, 281-290.
4. C.T. Yang and Y. Qi, Maintaining a Flat Li Surface during the Li Stripping Process via Interface Design, Chemistry of Materials, 2021, 33, 2814–2823
5. M.W. Swift, J.W. Swift, Y. Qi, Modeling the electrical double layer at solid-state electrochemical interfaces, Nature Computational Science 2021, 1, 212–220
6. Jung Hwi Cho, Kunjoong Kim, Srinath Chakravarthy, Xingcheng Xiao, Jennifer L. M. Rupp, and Brian W. Sheldon, "Investigation of chemo-mechanical phenomena in solid electrolytes using in-situ curvature measurements"

Patents

1. Xingcheng Xiao, Mengyuan Chen, Qinglin Zhang, Mei Cai, A solution-based approach to protect lithium metal electrode, P053352, US patent application
2. Xingcheng Xiao, Mengyuan Chen, Methods for Forming Ionically Conductive Polymer Composite Polymer Interlayers in Solid-state Batteries, GM Ref. No. P054138-US-NP
3. Mengyuan Chen, Xingcheng Xiao, Composite Interlayers for Solid State Batteries and the Method of Making Same, GM Ref. No. P054203-US-NP

Presentations

1. Brian W. Sheldon, Jung Hwi Cho, Christos E. Athanasiou, and Mok Yun Jin,, "Interface Stability and Related Chemo-Mechanical Phenomena During Lithium Metal Plating" Society of Engineering Science, October 2020 (Invited).
2. Jung Hwi Cho, Xingcheng Xiao, Kai Guo, Huajian Gao, & Brian W. Sheldon, "In Situ Investigations of Stress Evolution During Plating and Stripping of Lithium Metal", MRS, December 2020.
3. Jung Hwi Cho, Kai Guo, Huajian Gao, Xingcheng Xiao, and Brian W. Sheldon “Stress Evolution in Lithium Metal Electrodes and the Impact of Artificial Passivating Layers”, Pacific Rim Meeting on Electrochemical and Solid State Science, Oct. 2020 (virtual)

ACKNOWLEDGMENT

- Financial support from the Assistant Secretary for Energy Efficiency and Renewable Energy, Office of Vehicle Technologies, Advanced Battery Materials Research (BMR) programs of the U.S. Department of Energy (DOE) under contract no. DE-EE0008863
- Tien Duong, Tricia Smith, and Adrienne Riggi at DoE for program management
- Graduate students and postdocs: Mengyuan Chen (GM), Juny Cho, Min Feng (Brown) , Andrew Meyer (UK).
- Dr. Mei Cai, Dr. Mark W. Verbrugge, and Dr. Robert Schmitt for helpful discussion. Dr. Yun Cai for Micro-CT.

Back-up Slides

Anisotropic Curvature

Laser reflections oriented along the red dotted lines indicated below

Much larger bending (curvature) perpendicular to flaw line (i.e., highest curvature values at roughly 135 and 315 degrees

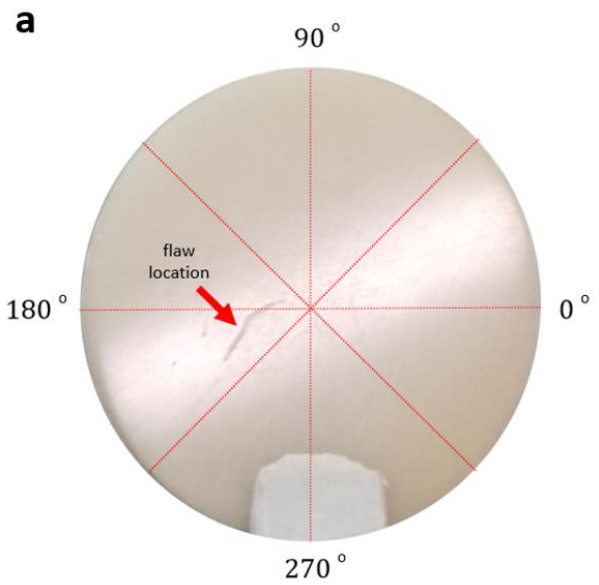

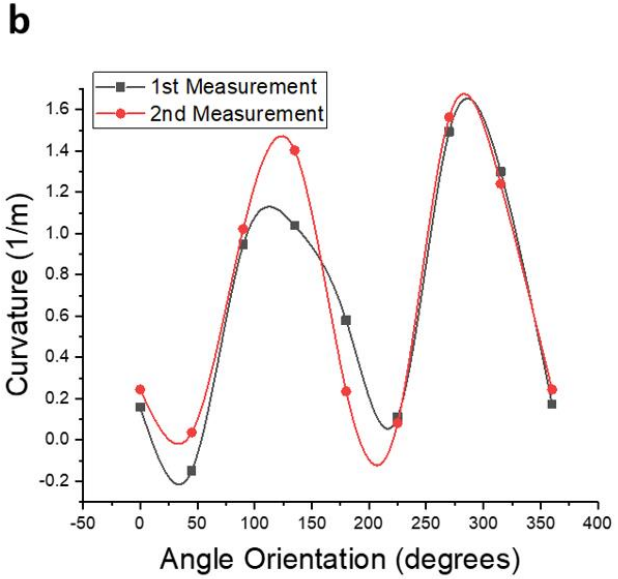

- Anisotropic curvature values at different angles w.r.t. to the surface flaw orientation are observed
- Supports the idea that the observations of curvature increase is closely correlated with partial lithium penetration (surface flaw is likely to accumulate more current and hence likely to initiate the crack propagation)

Task 1.1 – Develop a thin film platform for *in situ* experiments
Subtask 2.2.3 – Qualitatively understand the transport behavior of Li ion in model system:

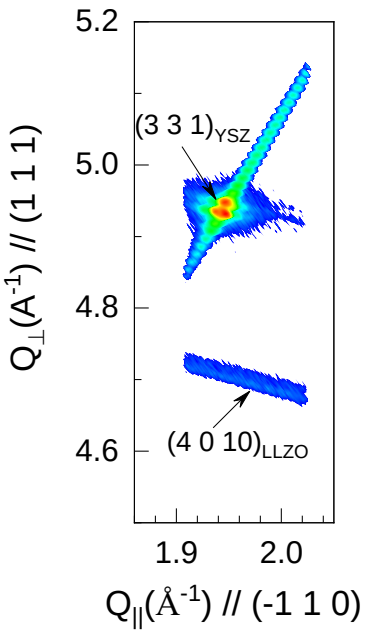

- **Question**: Can we create a thin film model system to study solid-state electrolytes (SSE's)?
- We successfully deposited LLZO thin films using Pulsed Laser Deposition (PLD) on various substrates such as YSZ(111), STO, and Stainless-steel.
- Reciprocal space mapping (RSM) to determine if the LLZO thin film is epitaxial in the all directions.
  - YSZ sample shows preferred crystal orientation in the z-direction (out-of-plane) but on in the x and y directions.
- Future work: Investigate different crystal orientations and compare various properties.
  - Ex. Ionic conductivity measurements by depositing *in situ* gold pads on LLZO thin films through a shadow mask to make conductive contact points for EIS measurements.

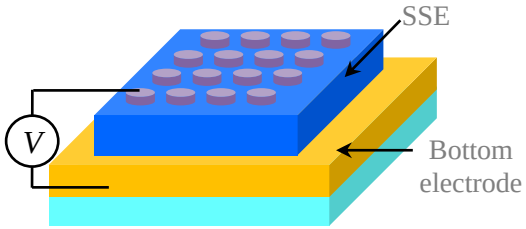

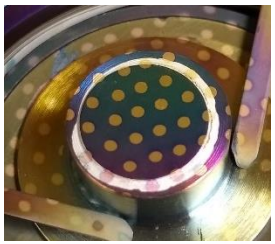

Stable Li_3N surfaces and its interface with Li

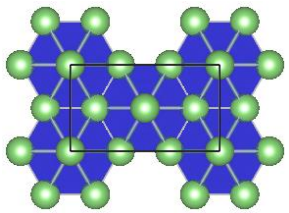

Top view of #1

#1

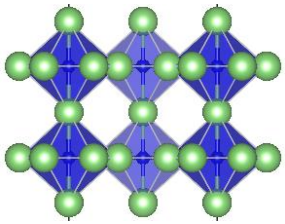

Li_3N (001)
Li terminated

#2

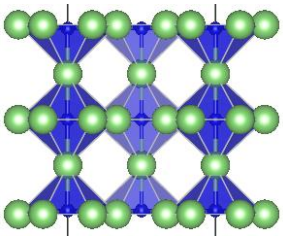

Li_3N (001)
Li, N terminated

Each N is coordinated by 8 Li, six on the same (001) plane (Li-N: 2.10 Å), one above and one below (Li-N: 1.95 Å).

Li: light green, N: blue.

#3

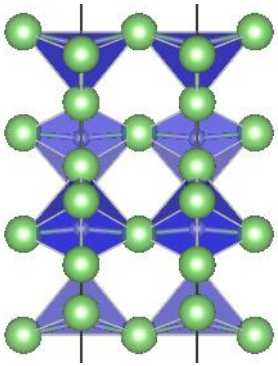

Li_3N (100)

#4

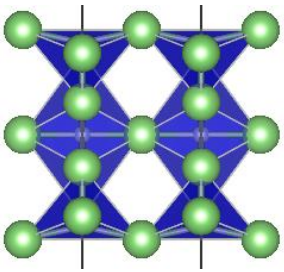

Li_3N (110)

$$C_{sur} = \frac{1}{2} * (C_{slab} - n * C_{bulk})$$

#	Surface	Formula	Termination (C_{sur})	Y (J/m^2)
1	Li_3N 001 Li	$Li_{14}N_4$	Li	0.54
2	Li_3N 001 Li, N	$Li_{16}N_6$	Li_2N	1.90
3	Li_3N 100	$Li_{10}N_4$	Li_2N	2.53
4	Li_3N 110	$Li_{14}N_6$	LiN	2.52

Slab	X-axis	Y-axis	θ(°)	In plane cells
Li (111)	14.5776	14.5776	120	3x3
Li_3N (001)	14.5544	14.5544	120	4x4
Strain	-0.16 %	-0.16 %	--	--

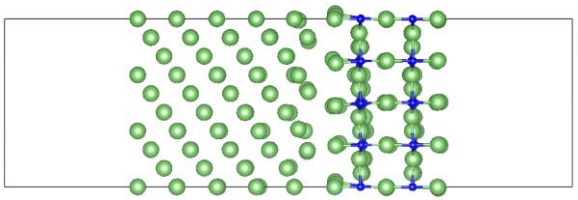

Li(111)/Li_3N (001) interface

Interface	Y_{interf} (J/m^2)	W_{adh} (J/m^2)	$Y_{Li(111)}$ (J/m^2)	cos(θ)	θ (°)
Li3N_001/Li_111	0.27	0.78	0.50	0.545	56.9

Developed a DFT-informed KMC model to simulate the vacancy evolution at Li/SE interfaces

DFT computed Li vacancy migration energy landscape

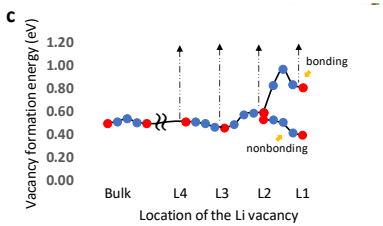

$$k = v_o \, exp\left(\frac{-\Delta E}{k_B T}\right)$$

Multi-events KMC model

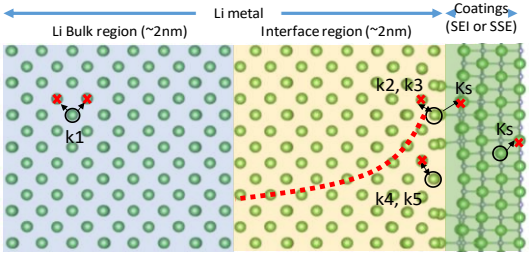

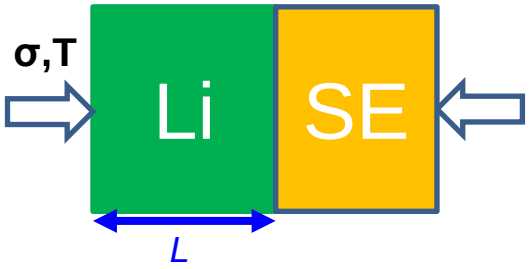

k	Diffusion Process	Li/Li_2O		Li/LiF	
		ΔE	k (300K)	ΔE	k (300K)
k_1	Bulk Li along [111]	0.045	1.74×10^{12}	0.045	1.74×10^{12}
k_2	Backward diffusion toward bulk for bonding Li atom migration L1→ L2	0.372	5.68×10^{6}	0	1.00×10^{13}
k_3	Forward diffusion toward interface involving bonding Li atom migration L2→ L1	0.156	2.43×10^{10}	0.331	2.68×10^{7}
k_4	Backward diffusion toward bulk for nonbonding Li atom migration L1→L2	0	1.00×10^{13}	0	1.00×10^{13}
k_5	Forward diffusion toward interface involving nonbonding Li atom migration L2→ L1	0.132	5.97×10^{10}	0.561	3.81×10^{3}
k_s	Removal of Li atoms in L1 due to stripping current density	NA	7.06 for 1.0 mA/cm^2	NA	8.00 for 1.0 mA/cm^2

(1) Correlate the Li diffusion flux rate ($\dot{n}$) with the strain rate ($\dot{\varepsilon}$(σ,T)) (assuming a Li foil of 100 um)

$$\dot{n} = \frac{N_A A_0 L \dot{\varepsilon}}{\bar{V}_{Li}}$$

(2) Make the flux rate equal to the net diffusion rates and solve the mechanical bias (E_p)

$$\dot{n} = k_f' - k_b'$$

$$\dot{n} = v_o \, exp\left(\frac{-E_f + 0.5E_p}{k_B T}\right) - v_o \, exp\left(\frac{-E_b - 0.5E_p}{k_B T}\right)$$

Define

$E_b' = E_b + 0.5E_p$ (Modified backward diffusion barrier)

$E_f' = E_f - 0.5E_p$ (Modified forward diffusion barrier)

Chi-Ta Yang and Yue Qi, Chemistry of Materials
https://doi.org/10.1021/acs.chemmater.0c04814

Accomplishment 4.1: developed a DFT-informed KMC model to simulate the vacancy evolution at Li/SE interfaces

BROWN School of Engineering

Qi's group

Relaxed Li/Li_2O interface & Li/LiF interface

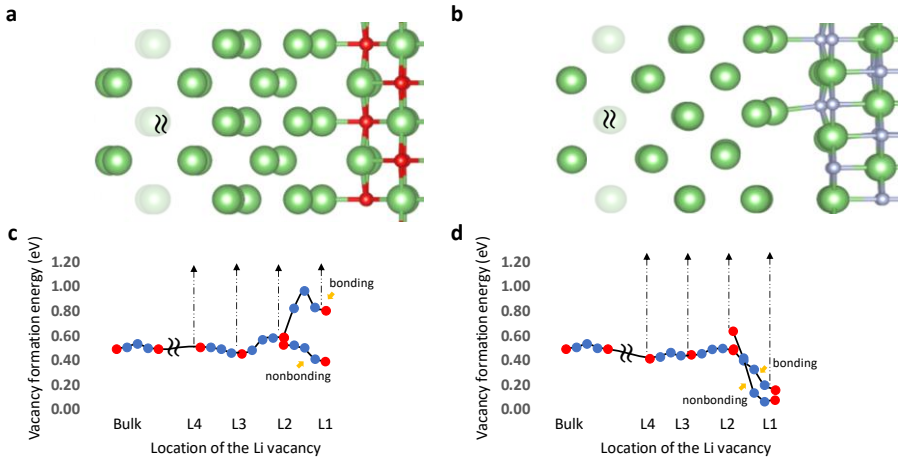

DFT computed Li vacancy migration energy landscape

Li/Li_2O interface:
Repels Li vacancy to the bulk
Attracts Li to the surface

Li/LiF interface:
Traps Li vacancy at the surface
Barrier for Li to fill the vacancy

Chi-Ta Yang and Yue Qi Chem. Mater. 2021, 33, 8, 2814–2823

Multi-events KMC model

$$k = v_o \, exp\left(\frac{-\Delta E}{k_B T}\right)$$

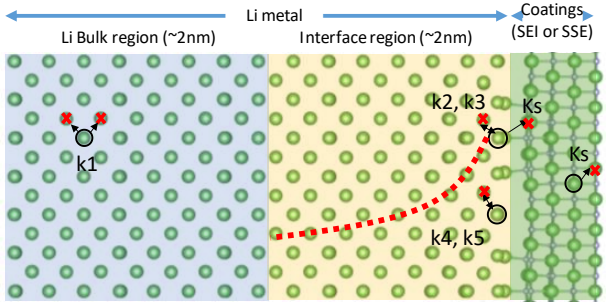

Li atom

k	Diffusion Process	Li/Li_2O		Li/LiF	
		ΔE	k (300K)	ΔE	k (300K)
k_1	Bulk Li along [111]	0.045	1.74×10^{12}	0.045	1.74×10^{12}
k_2	Backward diffusion toward bulk for bonding Li atom migration L1→ L2	0.372	5.68×10^{6}	0	1.00×10^{13}
k_3	Forward diffusion toward interface involving bonding Li atom migration L2→ L1	0.156	2.43×10^{10}	0.331	2.68×10^{7}
k_4	Backward diffusion toward bulk for nonbonding Li atom migration L1→L2	0	1.00×10^{13}	0	1.00×10^{13}
k_5	Forward diffusion toward interface involving nonbonding Li atom migration L2→ L1	0.132	5.97×10^{10}	0.561	3.81×10^{3}
k_s	Removal of Li atoms in L1 due to stripping current density	NA	7.06 for 1.0 mA/cm^2	NA	8.00 for 1.0 mA/cm^2